Magnetoresistance and Hall effect of $NbSi_2$ single crystals

2002 J. Phys.: Condens. Matter 14 7007

(http://iopscience.iop.org/0953-8984/14/29/302)

INSTITUTE OF PHYSICS PUBLISHING JOURNAL OF PHYSICS: CONDENSED MATTER

J. Phys.: Condens. Matter **14** (2002) 7007–7016 PII: S0953-8984(02)34881-1

Magnetoresistance and Hall effect of $NbSi_2$ single crystals

U Gottlieb[1], **O Laborde**[2] **and R Madar**[1]

[1] Laboratoire des Matériaux et du Génie Physique, Ecole Nationale Supérieure de Physique de Grenoble, Institut National Polytechnique de Grenoble, BP 46, 38042 Saint-Martin d'Hères, France

[2] Centre de Recherches sur les Très Basses Températures, Associé à l'Université Joseph Fourier, BP 166, 38042 Grenoble Cedex 9, France

Received 14 March 2002, in final form 10 June 2002
Published 11 July 2002
Online at stacks.iop.org/JPhysCM/14/7007

Abstract

We measured the transverse angular magnetoresistance and the Hall effect on high-quality $NbSi_2$ single crystals at low temperatures ($4.2\ \mathrm{K} \leqslant T \leqslant 160\ \mathrm{K}$) and high magnetic fields ($B \leqslant 20\ \mathrm{T}$). The material behaves like a compensated metal, i.e. the magnetoresistance grows generally proportionally to B^2. For some current–field configurations, however, saturation of the magnetoresistance occurs, giving evidence for the presence of an open orbit on the Fermi surface of $NbSi_2$ parallel to the c axis. The Hall coefficient shows, as does the magnetoresistance, a low-field–high-field transition. It varies between -3.5 and $-4.5 \times 10^{10}\ \mathrm{m^3\ C^{-1}}$ in low magnetic field to $-10.5 \times 10^{-10}\ \mathrm{m^3\ C^{-1}}$ in the high-field region. We compare our results with those obtained for $NbSi_2$ thin films and discuss the validity of parameters deduced from transport data.

1. Introduction

Transition-metal silicides are widely used in VLSI technology in thin-film form. The quantity of material is then very small and it is difficult to carry out experiments such as, for instance, specific heat or even magnetic measurements. Only transport properties can be easily studied on these samples. However, defects always present in the material dramatically affect these properties. The residual resistivity at low temperature is generally the same as the resistivity at room temperature, while for very pure single crystals the residual resistivity can be smaller by several orders of magnitude. The number and the nature of defects are difficult to control. The properties of the film such as epitaxy or disorder often depend on the substrate. Moreover, in some cases inter-diffusion between the silicide and the substrate can modify the stoichiometry of the material. This is one of the reasons why the sample properties can change by successive annealing after evaporation of the deposit. Transport measurements can therefore be viewed at first as a tool to roughly characterize thin films. To go deeper in data analysis, it is necessary

to know the intrinsic properties of the material, which can be obtained by measurements on very pure single crystals.

In the last few years we have developed a method to obtain high-quality single crystals of many silicides, allowing us to investigate a great variety of physical properties of transition-metal silicides [1]. $NbSi_2$ crystallizes in the hexagonal C_{40} structure (space group $P6222$). We have already studied many properties of $NbSi_2$ and the two related compounds VSi_2 and $TaSi_2$; notably, we have measured the resistivity [2], the low-temperature specific heat [3] and the magnetic susceptibility [4] of these disilicides.

The galvanomagnetic properties of single-crystalline metals measured under high magnetic field and at low temperatures have been widely used to investigate the electronic properties of pure metals. The magnetoresistance and Hall effect may provide important information about the Fermi surface topology [5, 6] and electronic parameters, such as carrier density, effective masses and scattering times.

In this paper we present the magnetoresistance and the Hall effect of high-quality single crystals of $NbSi_2$. The paper is organized as follows. In section 2 we describe briefly the sample preparation technique and the experimental set-up. In section 3 we present and discuss the obtained results, emphasizing the difficulties appearing during the determination of charge carrier density for a metal such as $NbSi_2$ with a complicated band structure. Finally we conclude.

2. Sample preparation and experimental details

High-quality single crystals of $NbSi_2$ were obtained by a modified Czochralski pulling technique from a levitated melt in a cold copper crucible. Details of the single-crystal fabrication process are described elsewhere [7]. We obtained two samples. The first one is a parallelepiped of dimensions $6 \times 3 \times 0.14$ mm^3, the longest dimension being parallel to the a axis and the shortest to the c axis. We shall call this sample sample a. It was used for magnetoresistance measurements for $I \parallel a$ and Hall effect measurements. The second sample was also a parallelepiped of dimensions $0.7 \times 0.7 \times 8$ mm^3; the longest sample dimension was aligned to the c axis. We shall call this sample sample c. This sample was used for magnetoresistance measurements with $I \parallel c$. The first sample is thin enough to obtain an easily detectable Hall voltage signal. In both cases, the precision of the sample alignment was about 1°. In this paper we shall call the crystallographic direction $[11\bar{2}0]$ the a axis, $[1\bar{1}00]$ the a^* axis and [0001] the c axis.

The high quality of the two samples was revealed by the residual resistance ratio (RRR $= \rho_{(300\ \mathrm{K})}/\rho_{(4.2\ \mathrm{K})}$). For sample a the RRR was higher than 1700 ($\rho_{(4.2\ \mathrm{K})} = 0.021\ \mu\Omega$ cm) and for sample c RRR $= 259$ ($\rho_{(4.2\ \mathrm{K})} = 0.085\ \mu\Omega$ cm). These values are very high for intermetallic compounds.

The resistivity is measured with a four-point ac method. The temperature regulation under magnetic field is achieved with a capacitor as a temperature detector. The field is produced either by a superconducting coil ($B \leqslant 7.8$ T) or by the resistive magnets of the High Magnetic Field Laboratory in Grenoble ($B \leqslant 20$ T). Electrical contacts are taken with aluminium wires of 20 μm in diameter, which are directly spot soldered on the sample. For resistivity measurements, current and voltage contacts are aligned along the longest sample dimension. For Hall measurements, Hall contacts are put perpendicular to the resistivity contact line on the border of the sample. The sample is mounted on a mechanical system which allows us to rotate it around an axis perpendicular to the field direction. This system is connected to a stepper motor controlled by a microcomputer. The rotation is detected by a device constructed in the laboratory. The resolution of the rotation obtained is better than 0.1°. Care is taken to align

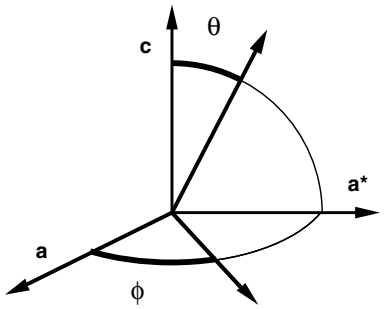

Figure 1. Angle definition for the measurements of the angular dependence of the magnetoresistivity.

the longest sample dimension with the rotation axis. Thus the current is always perpendicular to the magnetic field. The experimental set-up allows us to measure the magnetoresistance at fixed temperature:

(i) for a constant magnetic field as a function of the field orientation relative to the crystallographic axis or
(ii) for a given field orientation as a function of magnetic field strength.

The representation data points in figures are an average of many measured experimental points.

In figure 1, we present the angles between the magnetic field and the crystallographic axes that we used for our magnetoresistance measurements. The field is always perpendicular to the current. For $I \parallel a$ the field is applied in the a^*–c plane and θ is the angle between the c axis and the field. For $I \parallel c$, the field is applied in the a–a^* plane and φ is the angle between the a axis and B. The Hall effect between 4.2 and 160 K was measured on sample a, i.e. $I \parallel a$ and $B \parallel c$. The Hall voltage was measured parallel to a^*, perpendicular to the current and the field. The Hall voltages V^+ and V^- were systematically measured for the two opposite directions of the magnetic field, and we used $V_H = (V^+ - V^-)/2$ in order to eliminate the spurious voltage resulting from a possible misalignment of the contacts.

3. Results and discussion

3.1. Magnetoresistance

The magnetoresistance is caused by the bending of the carrier trajectories on the Fermi surface by the Lorentz force under the influence of an applied magnetic field. In the low-magnetic-field limit, i.e. $\omega_C\tau \ll 1$ (ω_C is the cyclotron frequency and τ the scattering time of charge carriers; $\omega_C\tau$ corresponds to the number of orbits that charge carriers can make on the Fermi surface before being scattered), $\Delta\rho/\rho$ is proportional to B^2 [6]. In the case of a compensated metal (charge carriers are electrons and holes with equal numbers) and in supposing that both types of carrier have equal mobilities, $\Delta\rho/\rho = (\omega_C\tau)^2$ up to highest fields, allowing an estimation of $\omega_C\tau$. In the high-field limit, $\omega_C\tau > 1$, however, the behaviour of $\Delta\rho/\rho$ depends on the topology of the Fermi surface [6]. For compensated metal, the occurrence of saturation of $\Delta\rho/\rho$ for particular field and current directions indicates the presence of an open orbit perpendicular to B and I [5]. In normal metals, the transverse magnetoresistance follows a Kohler law:

$$\frac{\Delta\rho}{\rho} = \frac{\rho(B) - \rho(B=0)}{\rho(B=0)} = f\left(\frac{B}{\rho}\right), \tag{1}$$

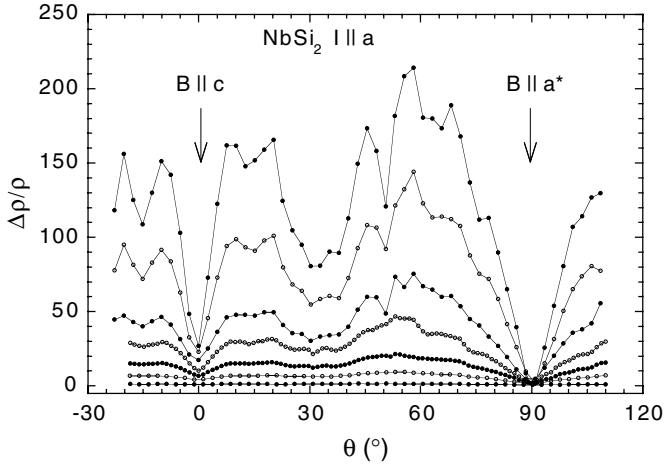

Figure 2. Transverse magnetoresistance of $NbSi_2$ at 4.2 K for $I \parallel a$ as a function of the field direction for $B = 1$, 3, 5, 7.5, 10, 15 and 20 T.

where f is a characteristic function for the metal of the reduced variable B/ρ. B/ρ is proportional to $\omega_C\tau$.

In figure 2, we present the transverse magnetoresistance of $NbSi_2$ at 4.2 K for the current parallel to the a axis and for magnetic fields of 1, 3, 5, 7.5, 10, 15 and 20 T as a function of the field direction. For low field ($B = 1$ T) $\Delta\rho/\rho$ is nearly isotropic. At higher fields, an important anisotropy appears, reproducing the twofold crystal symmetry in the a^*–c plane. For $B = 20$ T, $\Delta\rho/\rho$ is generally very high ($\Delta\rho/\rho \approx 100$–200), with the exception of some field directions. We can estimate $\omega_C\tau \approx 10$–15 for sample a, so we are clearly in the high-field limit for a field of 20 T.

In figure 3, we present $\Delta\rho/\rho$ as a function of magnetic field strength for some characteristic field directions. The label 'max' indicates an angle $\theta = 57°$, where the magnetoresistance of figure 2 is the highest one. As one can see in figure 3, for $B \parallel a^*$, $\Delta\rho/\rho$ saturates at low field and remains practically constant up to 20 T. For $B \parallel \max\Delta\rho/\rho$ varies nearly proportionally to B^2 up to the highest field, and for $B \parallel c$ the magnetoresistance shows an intermediate behaviour.

In figure 4, we present the magnetoresistance at 4.2 K for $I \parallel c$ for magnetic fields of 1, 3, 5 and 7.5 T as a function of the field direction. It is important to notice that the y scale is enhanced by a factor of ten relative to that of figure 2. The fact that the magnetoresistance of sample c is lower than that of sample a can be explained by two factors:

(a) the residual resistivity of sample c is four times higher than that of sample a and
(b) for the measurements with $I \parallel c$ the maximum field was only 7.8 T whereas it was 20 T for measurements of sample a.

For $I \parallel c$ (figure 4), $\Delta\rho/\rho$ is nearly isotropic in low field ($B = 1$ T). At higher fields, small variations of the magnetoresistance occur, but they are less important than the variations observed in the magnetoresistance with $I \parallel a$. Nevertheless, the magnetoresistance of sample c reflects the sixfold symmetry of the a–a^* plane of the crystal structure. We can estimate $\omega_C\tau \approx 4$ for this sample at 7.5 T, so we can conclude that we have also reached the high-field limit with sample c at 7.5 T. This value has to be compared with $\omega_C\tau \approx$ 6–7 for sample a at the same field strength.

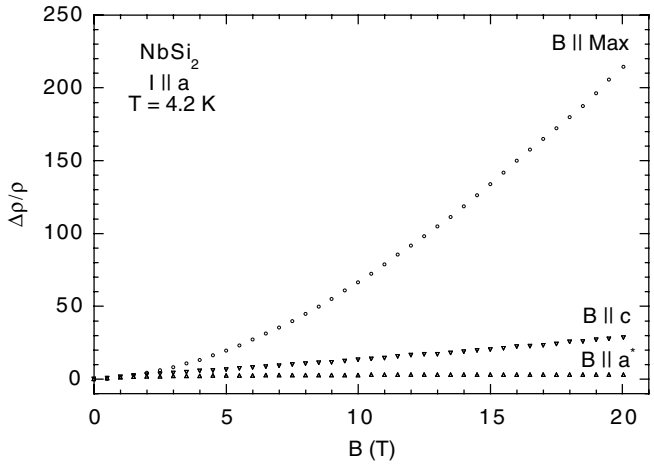

Figure 3. Magnetoresistance as a function of B for some characteristic field directions with $I \parallel a$.

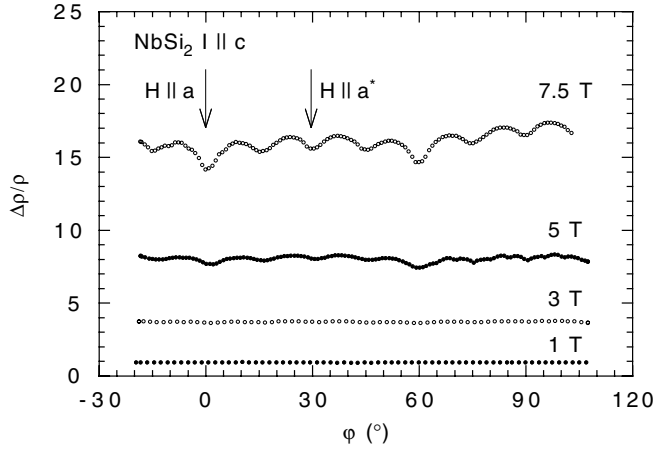

Figure 4. Transverse magnetoresistance of $NbSi_2$ at 4.2 K for $I \parallel c$ as a function of the field direction for $B = 1$, 3, 5 and 7.5 T.

In figure 5, we present $\Delta\rho/\rho$ versus magnetic field strength for two characteristic field directions. The label 'max' indicates an angle $\varphi = 7.5°$, in one of the small maxima of the magnetoresistance in figure 4. In figure 5, one can see that $\Delta\rho/\rho$ varies nearly proportionally to B^2 up to the highest fields in both cases.

The magnetoresistance of $NbSi_2$ varies as B^2 for nearly all field–current configurations. This indicates that $NbSi_2$ behaves like a compensated metal. We have already observed a compensated metal behaviour in the case of $TaSi_2$ [2] and Pd_2Si [8]. The saturation of the magnetoresistance we observe for $I \parallel a$ and $B \parallel a^*$ indicates the presence of an open orbit on the Fermi surface of $NbSi_2$. This open orbit is parallel to the c axis. We have to note a small trend toward saturation for $B \parallel c$ in figure 2 and $B \parallel a$ in figure 4, which could result from an open orbit parallel to the a^* direction, but the effect is not evident enough to make any conclusions.

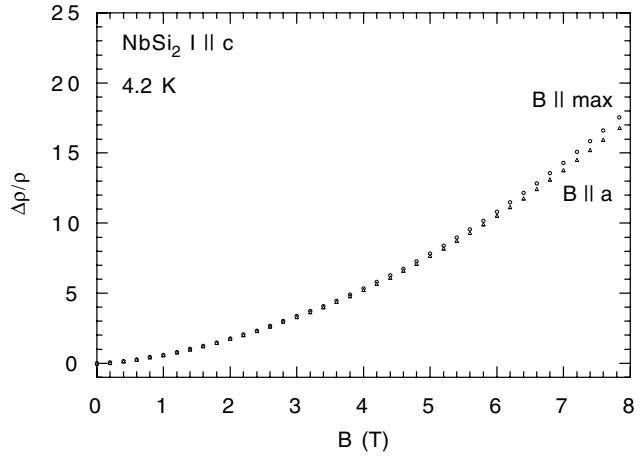

Figure 5. Magnetoresistance as a function of B for some characteristic field directions with $I \parallel c$.

Some band structure calculations of $NbSi_2$ are available in the literature but details of the topology of the Fermi surface is not known [9]. Recent results show that the Fermi surface of $NbSi_2$ is of a very complex geometry and the presence of an open orbit seems possible along the c direction [10].

In figure 6, we present a Kohler plot (log–log diagram of $\Delta\rho/\rho$ versus B/ρ) of the magnetoresistance for temperatures between 4.2 and 160 K for $I \parallel a$ and different field orientations. For a given field orientation, Kohler's law is very well obeyed as the curves taken at different temperatures show an excellent superposition. By temperature and field variation, B/ρ is modified over by more than four orders of magnitude, and the magnetoresistance varies by over five orders of magnitude. In the low-field limit ($\Delta\rho/\rho < 1$), Kohler's law is even well obeyed for any field direction.

In this limit, data are well described by the expression

$$\Delta\rho/\rho = 4 \times 10^{-18}(B/\rho)^2,$$

where B is in tesla and ρ in Ω m (see curves).

At high values of B/ρ this law is no longer valid, because of the occurrence of saturation as for $B \parallel a^*$; or even for $B \parallel$ max a change in the slope of the curve appears. This is a result of the transition between the low- and high-field regimes. This transition occurs for $B/\rho \approx 10^9$ T Ω^{-1} m^{-1}. The corresponding value of the magnetoresistance is nearly unity as expected for $\omega_C\tau = 1$.

3.2. Hall effect

In figure 7, we have plotted the Hall voltage divided by the current, V_H/I, as a function of the magnetic field for some characteristic temperatures between 4.2 and 160 K. For all measured temperatures the Hall voltage is negative, indicating that electrons are the dominant charge carriers. At high temperature V_H/I varies linearly with B up to 7.8 T. At 4.2 K, V_H/I shows a curvature at $B \leqslant 1$ K. For 40 and 48 K, we can also observe this curvature but at higher values of the field. We can observe two limits in the behaviour of V_H/I.

At low magnetic field and for temperatures below 50 K, V_H/I varies proportionally to B with nearly the same slope as curves measured at high temperature. At high field, V_H/I

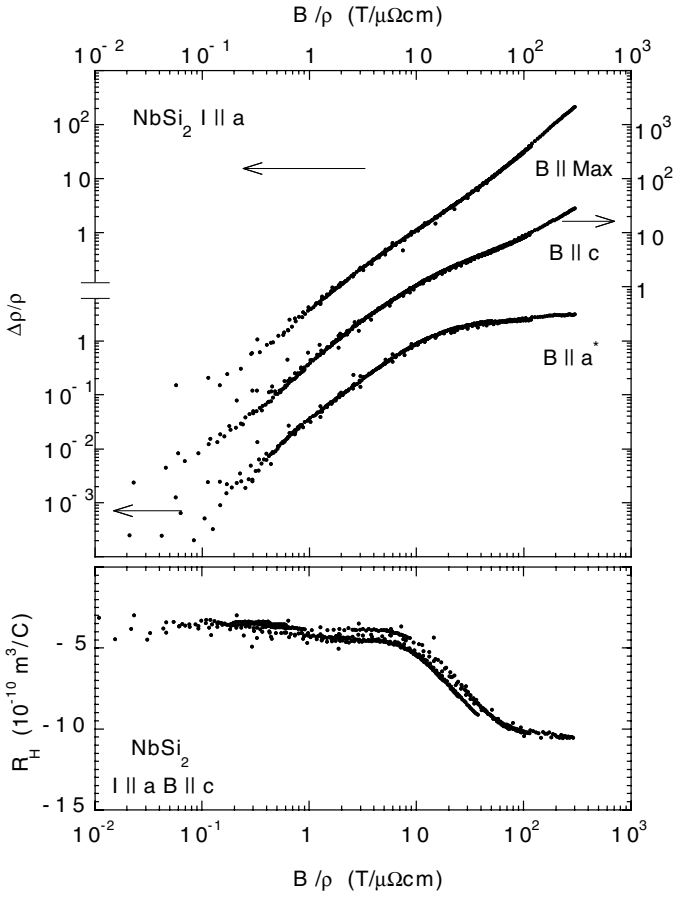

Figure 6. Kohler plots of the transverse magnetoresistance and the Hall effect of $NbSi_2$.

also varies linearly with B but with a higher slope. The magnetic field necessary to pass from one limit to the other increases with the temperature. This behaviour suggests that the Hall coefficient $R_H = \rho_H/B = V_H t/IB$ (where ρ_H is the Hall resistivity and t is the thickness of the sample) will also follow a Kohler law.

In figure 6, we have plotted R_H as a function of B/ρ with the same x-scale as the magnetoresistance results. Data at 4.2 K and up to 20 T, not shown for clarity in figure 7, are plotted in figure 6. R_H follows a Kohler law as does the magnetoresistance. It varies between two limiting values: $R_H \approx -3.5$ to -4.5×10^{-10} m^3 C^{-1} in the low-field limit and $R_H \approx -10.5 \times 10^{-10}$ m^3 C^{-1} in the high-field limit. The curvature of V_H/I observed in figure 7 corresponds to a transition between the low- and high-field limits.

In the low-field limit R_H shows a small temperature variation, as can be seen in figure 8. The fact that we can observe the low-field limit only in a small field range at low temperatures is at the origin of a large uncertainty on the data in that temperature range. This temperature variation explains the small deviations from a Kohler law of the Hall coefficient observable at low B/ρ value in figure 6.

The transition between a low-field value and a high-field value of the Hall constant has mainly been observed in pure metals. It can lead to large variation for R_H with even a change

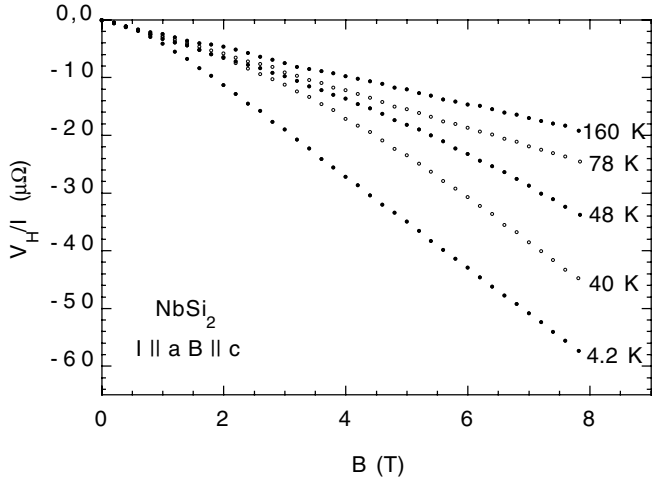

Figure 7. Hall voltage divided by the current versus B for some characteristic temperatures.

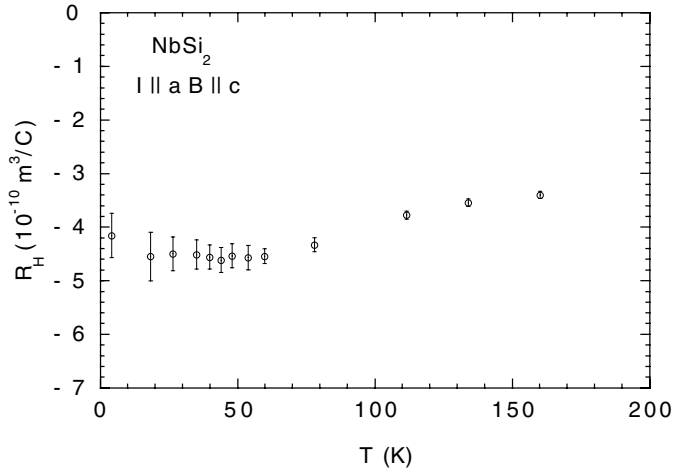

Figure 8. Low-field variation of R_H as a function of temperature.

in sign for aluminium between the two regimes [9]. In the high-field limit R_H is related to the topology of the Fermi surface, as charge carriers can make a great number of orbits before being scattered. In the low-field limit the charge carriers are scattered after having explored only a small part of the Fermi surface. In this case R_H is also dependent on the scattering mechanisms [11].

One can also write $\omega_C\tau$ as a function of the transport parameters [6]:

$$\omega_C\tau = \frac{R_H}{\rho}B. \tag{2}$$

With equation (1), using $R_H = -10.5 \times 10^{-10}$ m^3 C^{-1} in the high-field limit, $\omega_C\tau = 1$ corresponds to $B/\rho \approx 10^9$ T Ω^{-1} m^{-1}. As can be clearly seen in the Kohler plot of figure 6, the magnetoresistance and the Hall coefficient show the transition between the low-field and the high-field limits at this value of B/ρ.

Previous measurements of the Hall effect of $NbSi_2$ had been obtained on polycrystalline thin-film samples [12]. The resistivity of these films was high, and the experiments were performed at high temperature under magnetic fields up to 1.5 T, so these measured values of the Hall effect correspond to the low-field limit value. They are in good agreement with our results as long as the film is excess-silicon free.

In the case of a metal in which the conductivity is dominated by a high-mobility band of carriers, the following approximation is often used for the magnetoresistance [13]:

$$\Delta\rho/\rho = (\mu_M B)^2,$$

where μ_M is an effective magnetoresistance mobility. If $\sigma = 1/\rho = ne\mu$, we can deduce in that approximation an effective carrier concentration from the quadratic low-field variation of the magnetoresistance

$$\Delta\rho/\rho = (1/ne)^2(B/\rho)^2.$$

With the experimental value we obtain $1/n|e| = 20 \times 10^{-10}$ m^3 C^{-1} and $n = 0.31 \times 10^{28}$ carriers m^{-3}. From the Hall measurement, with a simple free-electron model, $R_H = 1/ne$, we can estimate $n = 0.59 \times 10^{28}$ electrons m^{-3} in the high-field limit, a value twice as large as the previous one. In the low-field limit, n obtained in this way from R_H is otherwise five times larger than that estimated from the magnetoresistance analysis. This underlines the difficulties encountered in calculating the carrier concentration from Hall effect measurements using an over-simplified model in the case of a compound which has a rather complicated electronic band structure. Moreover, for thin films we are always in the low-field limit because of their film residual resistance values.

These results indicate that we have to be careful with parameters deduced from transport data, particularly in the case of thin films. However, if these measurements can be performed in a large range of temperature and magnetic field on well characterized samples, they are a powerful tool to investigate metallic compounds.

4. Conclusion

We have measured the magnetoresistance and the Hall effect of $NbSi_2$ high-quality single crystals. The Hall effect and the magnetoresistance both follow a Kohler law. Our results show clearly the transition between a low-field and a high-field limits. This was achieved because we had at our disposal samples with very high RRR and very large magnetic fields.

The magnetoresistance of $NbSi_2$ shows the behaviour of a compensated metal. The transverse magnetoresistance as a function of the field direction relative to the crystallographic axes reproduces the crystal symmetry. The results indicate the presence of an open orbit on the Fermi surface of $NbSi_2$ parallel to the c axis. The Hall coefficient remains negative in the whole explored temperature range. It varies by a factor larger than two between the low-field and the high-field limits. These new results together with the previous ones for $NbSi_2$ should now stimulate detailed calculations to be compared with the experimental data.

Acknowledgment

This work was financially supported by the European Community in the framework of the programme ‘Human capital and mobility’, contract number ERBCHRXTCT930318.

References

[1] Gottlieb U, Nava F, Affronte M, Laborde O and Madar R 1995 *Metal Silicides (EMIS Datareviews Series No 14) INSPEC* ed K Maex and M Van Rossum ch 5

[2] Gottlieb U, Laborde O, Thomas O, Rouault A, Sénateur J P and Madar R 1991 *Appl. Surf. Sci.* **53** 247

[3] Lasjaunias J C, Laborde O, Gottlieb U, Madar R and Thomas O 1993 *J. Low Temp. Phys.* **92** 335

[4] Gottlieb U, Sulpice A, Madar R and Laborde O 1993 *J. Phys.: Condens. Matter* **5** 8755

[5] Fawcett E 1964 *Adv. Phys.* **13** 139

[6] Pippard A B 1989 *Magnetoresistance in Metals* (Cambridge: Cambridge University Press)

[7] Thomas O, Sénateur J P, Madar R, Laborde O and Rosencher E 1985 *Solid State Commun.* **55** 629

[8] Laborde O, Gottlieb U and Madar R 1994 *J. Low Temp. Phys.* **95** 835

[9] Carlsson A E and Meschter P J 1991 *J. Mater. Res.* **6** 1512

[10] Antonov V N, Yavorsky B Yu, Shpak A P, Antonov Vl N, Jepsen O, Guizetti G and Marabelli F 1996 *Phys. Rev.* B **53** 15 631

[11] Hurd C M 1972 *Hall Effect in Metals and Alloys* (New York: Plenum)

[12] Pomoni K, Krontiras Ch and Salmi J 1990 *J. Phys. D: Appl. Phys.* **23** 354

[13] Huang M T, Martin T L, Malhotra V and Mahan J E 1985 *J. Vac. Sci. Technol.* B **3** 836